

Electron dynamics in laser and quasi-static transverse electric and longitudinal magnetic fields

Yanzeng Zhang and S. I. Krasheninnikov
University of California San Diego, 9500 Gilman Dr., La Jolla, CA 92095

E-mail: yaz148@eng.ucsd.edu

Abstract.

By deriving the 3/2 dimensional Hamiltonian method for electrons in the intense laser radiation and quasi-static transverse electric and longitudinal magnetic fields, the electron heating mechanisms are examined both for low harmonic resonance of electron frequency in the static fields with the laser frequency and for high harmonic resonances where the overlap of broadened resonances causes the stochastic heating. In the former case, it shows that the efficient electron heating is only possible for the first harmonic resonance where the electron gyrofrequency in the strong longitudinal magnetic field is matching the laser frequency. In the latter case it demonstrates that the stochasticity is weakened due to the presence of weak magnetic field which will terminate the stochastic heating when exceeding a critical strength. The maximum electron energies in the measurement of ponderomotive scaling in both cases are shown to only depend on a small parameter combining the laser amplitude, electrostatic field strength and initial condition.

1. Introduction

The plasma interactions with intense laser radiation open up possibilities for many interesting and important applications, including generation of intense X-ray radiation, energetic electron and ion beams, positrons production, etc. and have been intensively studied over the years (see e.g. [1-19] and the references therein). Relatively recently it was shown that the presence of self-generated or externally applied quasi-static electric and magnetic fields could significantly facilitate the laser plasma coupling and play a very beneficial role for many different reasons in the electron acceleration well beyond the ponderomotive scaling. Although the maximum electron energy has been estimated in some of these studies (e.g., see [4, 8-9, 12-16]) as a function of the parameters of the laser radiation and static electromagnetic fields through simplified analyses and numerical simulations, the underlying synergistic mechanism(-s) of the laser and these static electromagnetic fields is still difficult to assess due to the strong nonlinearity of the relativistic electron dynamics in these fields.

However, in [20-23] it was shown that the electron dynamics in an arbitrarily polarized laser radiation and arbitrary quasi-static electric fields in the directions both aligned with (longitudinal) and crossed to (transverse) the laser propagation direction as well as arbitrary transverse magnetic field can be described by the 3/2 dimensional (3/2D) Hamiltonian approach, which greatly simplifies the analysis of electron interactions with laser and quasi-static electromagnetic fields. It was demonstrated [21-23] that, in the presence of quasi-static electromagnetic fields, the acceleration of electron is attributed to an onset of stochasticity [24-25].

In the present paper, the 3/2D Hamiltonian approach is extended to the case of electron interactions with arbitrary longitudinal magnetic and transverse electric fields, within which the electron dynamics shall be investigated. Following [21-23], we will use the dimensionless variables $\hat{t} = t\omega$, $\hat{\mathbf{r}} = k\vec{r}$, $\hat{\mathbf{v}} = \vec{v}/c$, $(\hat{\mathbf{A}}, \hat{\mathbf{A}}_B) = e(\vec{A}, \vec{A}_B)/m_e c^2$ and $\hat{U} = eU/m_e c$, where e is the elementary charge, m_e is the electron mass and c is the speed of light in vacuum; ω and k are, respectively, the frequency and wave number of the laser radiation; \vec{A} is the laser vector potential; U and A_B are the quasi-static electric and magnetic vector potentials, respectively. In what follows we will remove the hats over the normalized variables to simplify our expressions.

The remainder of the paper is organized as follows. In section 2 we derive the 3/2D Hamiltonian of the electron in the laser pulse and transverse electric and longitudinal magnetic fields. Section 3 will discuss the electron trajectories in these static fields with an impact of the laser radiation. The electron dynamics for weak static fields is examined in section 4, where overlap of the broadened high harmonic resonances of electron frequency with the laser frequency would result in stochastic electron heating. While for a strong magnetic field, the efficient electron heating presented in section 5 is possible via single low harmonic resonance. Section 6 will summarize the main results.

2. 3/2D Hamiltonian for electron in longitudinal magnetic and transverse electric fields

In this section, we derive the 3/2D Hamiltonian for electron in the electromagnetic field described by the vector potential in the form of

$$\vec{A} = \vec{A} - \vec{e}_y t \partial U(y) / \partial y + \vec{e}_x A_B(y), \quad (1)$$

where the quasi-static electric, $U(y)$, and magnetic vector, $A_B(y)$, potentials depend only on the coordinate y , whereas arbitrarily polarized laser wave is expressed by the vector potential $\tilde{A} = \tilde{A}_x(\xi)\tilde{e}_x + \tilde{A}_y(\xi)\tilde{e}_y$ with $\tilde{A}_x(\xi)$ and $\tilde{A}_y(\xi)$ being arbitrary functions of the variable $\xi \equiv t - z/\alpha$ and $\alpha = v_{ph}/c \geq 1$ the normalized laser phase velocity. Then, it is easy to show that there are two integrals of electron motion

$$\bar{P}_x \equiv P_x - (\tilde{A}_x + A_B), \quad (2)$$

$$C_\perp \equiv \gamma - \alpha P_z + U(y). \quad (3)$$

Introducing the variable $\tilde{p}_y = P_y - \tilde{A}_y$, after some algebra similar to that in [22], the 3/2D Hamiltonian equations read

$$\frac{d\tilde{p}_y}{d\xi} = -\frac{\partial H}{\partial y}, \text{ and } \frac{dy}{d\xi} = \frac{\partial H}{\partial \tilde{p}_y}, \quad (4)$$

where

$$H(\tilde{p}_y, y, \xi) = \frac{\alpha}{\alpha^2 - 1} \left\{ \sqrt{(U - C_\perp)^2 + (\alpha^2 - 1)P_{\perp,y}^2} + \alpha U - C_\perp \right\} \equiv \gamma + U - \frac{C_\perp}{\alpha + 1}, \quad (5)$$

and

$$P_{\perp,y}^2 = 1 + (\bar{P}_x + \tilde{A}_x + A_B)^2 + (\tilde{p}_y + \tilde{A}_y)^2. \quad (6)$$

Notice that the Hamiltonian in equation (5) corresponding to the luminal phase velocity $\alpha \rightarrow 1$ becomes

$$H = \frac{1}{2} \left\{ \frac{1 + (\bar{P}_x + \tilde{A}_x + A_B)^2 + (\tilde{p}_y + \tilde{A}_y)^2}{C_\perp - U(y)} + U(y) \right\} \equiv \gamma + U(y) - \frac{C_\perp}{2} = P_z + \frac{C_\perp}{2}. \quad (7)$$

The strongest interaction between the electron and laser wave occurs for the case where electron stays in phase with the laser wave, which implies small difference $\gamma - P_z$. However, from Eq. (3) we have $\gamma - P_z = C_\perp - U(y) + (\alpha - 1)P_z$, which indicates that whereas static electric field could enhance the electron-laser interaction when U approaches C_\perp , the superluminal phase velocity of laser radiation, $\alpha > 1$, would reduce it [4, 21, 22].

For simplicity, in this paper we consider luminal case, $\alpha = 1$, and assume that $\bar{P}_x = 0$. To specify static transverse electric and longitudinal magnetic fields we take $U = \kappa y^2/2$ and $A_B = B_0 y$ where κ and B_0 are some constants. Moreover, we will analyze linear laser polarization and take either $\tilde{A} = a_0 \sin(\xi)\tilde{e}_y$ or $\tilde{A} = a_0 \sin(\xi)\tilde{e}_x$ where a_0 is the normalized amplitude of laser vector potential.

3. Electron trajectories and an impact of the laser radiation

First we consider electron trajectory neglecting an impact of the laser field. Then, our Hamiltonian (7) is conserved, $H = E = \text{const.}$ (where E is electron energy), and from Eqs. (4, 7) we find

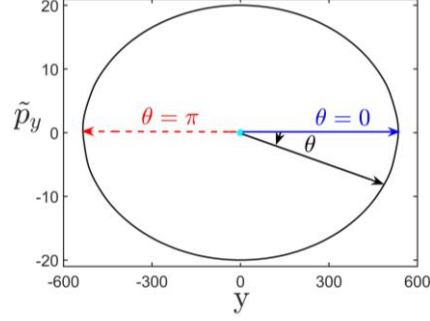


Fig. 1. Schematic view of the ultrarelativistic electron trajectory on (\tilde{p}_y, y) plane for $C_\perp = 1$, $\kappa = 10^{-5}$, $B_0 = 0.02$ and $E = 100$.

$$y = \sqrt{2EC_\perp(\kappa E + B_0^2)^{-1}} \cos \theta, \quad \tilde{p}_y = -\sqrt{2EC_\perp} \sin \theta, \quad (8)$$

where angle θ , which goes in a clockwise direction as shown in Fig. 1 with $\theta = 0$ ($\theta = \pi$) corresponding to maximum (minimum) of the coordinate y : $y = y_{\max}$ ($y = y_{\min}$), is determined by the following equation

$$\frac{d\theta}{d\xi} = \frac{(\kappa E + B_0^2)^{3/2}}{(B_0^2 + \kappa E \sin^2 \theta)C_\perp}. \quad (9)$$

From Eq. (9) we find

$$\zeta \equiv \xi - \xi_{\max} = \frac{C_\perp}{(\kappa E + B_0^2)^{3/2}} \left[B_0^2 \theta + \frac{2\theta - \sin(2\theta)}{4} \kappa E \right], \quad (10)$$

where ξ_{\max} is the “time” of the passage of the electron through $y = y_{\max}$. Substituting $\theta = 2\pi$ in the above expression yields the frequency of unperturbed electron motion over closed orbit

$$\Omega = \frac{(\kappa E + B_0^2)^{3/2}}{C_\perp} \left(B_0^2 + \frac{\kappa E}{2} \right)^{-1}. \quad (11)$$

The same result could be derived from the calculation of the action, I , of the electron from Eq. (8,9), which gives $I = \oint \tilde{p}_y dy / 2\pi = EC_\perp(\kappa E + B_0^2)^{-1/2}$, and $\Omega = \partial E / \partial I$ results in the expression (11).

However, analyzing Eq. (7) we find that an impact of laser radiation on electron trajectory could be largely ignored (with exception rather narrow regions in the vicinity of $\theta = 0$ and $\theta = \pi$, where \tilde{p}_y approaches zero) only for the energies

$$E > E_{\text{pond}} = a_0^2 / 2C_\perp, \quad (12)$$

where E_{pond} in our case could be considered as a ponderomotive energy scaling.

Recalling that according to our normalization convention, frequency Ω is normalized to the laser frequency, we conclude that for efficient electron-laser interactions the frequency Ω (or its harmonics) should either be in a resonance with laser frequency, which implies $n\Omega = 1$ (where $n \geq 1$ is the integer number), or resonance broadening should result in the overlap of the resonances, which causes stochastic electron heating [24, 25]. Thus, the requirement $\Omega \leq 1$ sets the limit for efficient electron-laser interactions since at $\Omega > 1$ an impact of laser field becomes adiabatic.

From Eq. (11) one could see that the inequality $\Omega > 1$ could be reached when either B_0 or E or both are large. However, for

$$B_0 > C_{\perp} \quad (13)$$

we find that $\Omega > 1$ at any values of E , whereas for

$$E > E_{\max}^{\text{abs}} = C_{\perp}^2 / 4\kappa, \quad (14)$$

it appears that $\Omega > 1$ at any value of B_0 . Thus, E_{\max}^{abs} could be considered as an absolute maximum energy where electron could be heated up via interactions with the laser radiation. From Eq. (12, 14) we find that in order to be able to heat electrons beyond ponderomotive scaling, we should have

$$\varepsilon \equiv \sqrt{2}a_0\kappa^{1/2}C_{\perp}^{-3/2} < 1, \quad (15)$$

where $E_{\max}^{\text{abs}} = E_{\text{pond}}\varepsilon^{-2}$. In what follows, we would use E_{\max}^{abs} to scale the electron energies.

Electron energy variation due to an impact of the laser radiation is $E(\xi) = \int^{\xi} (\partial H / \partial \xi) d\xi$ and for $\tilde{\mathbf{A}} = a_0 \sin(\xi) \vec{e}_y$ and $\tilde{\mathbf{A}} = a_0 \sin(\xi) \vec{e}_x$ we have, correspondingly:

$$E_y(\xi) - E_y(\xi_{\max}) = \int_{\xi_{\max}}^{\xi} \frac{a_0(a_0 \sin \xi + \tilde{p}_y) \cos \xi}{C_{\perp} - U(y)} d\xi, \quad (16a)$$

and

$$E_x(\xi) - E_x(\xi_{\max}) = \int_{\xi_{\max}}^{\xi} \frac{a_0[a_0 \sin \xi + A_B(y)] \cos \xi}{C_{\perp} - U(y)} d\xi. \quad (16b)$$

4. High-n resonances and stochastic electron heating

First we consider Eq. (16) for the case where $\Omega \ll 1$ (the static fields satisfying $\kappa E + B_0^2 \ll C_{\perp}^2$) and electron heating is due to overlapping of high-n resonances ($n\Omega = 1$). For this case we follow [23] and consider electron energy change during relatively short time of strong interactions of electron with laser radiation (we will call them ‘‘collisions’’) in the vicinity of $y = y_{\max}$ and $y = y_{\min}$. We assume that electron energy variation during such collisions, ΔE , is small $|\Delta E| \ll E$ such that the unperturbed electron trajectories in equations (8, 9) can be applied to assess the electron energy change between two consecutive collisions from Eq. (16), i.e.,

$$\Delta E_y = a_0 \left(\frac{2EC_{\perp}}{\kappa E + B_0^2} \right)^{1/2} \sin \xi_j \int_{-\pi/2}^{\pi/2} \sin \theta \sin \left[\frac{\theta}{\Omega_B} + \frac{2\theta - \sin(2\theta)}{4\Omega_E} \right] d\theta + \frac{a_0^2}{2(\kappa E + B_0^2)^{1/2}} \sin(2\xi_j) \int_{-\pi/2}^{\pi/2} \cos \left[\frac{2\theta}{\Omega_B} + \frac{2\theta - \sin(2\theta)}{2\Omega_E} \right] d\theta, \quad (17a)$$

$$\Delta E_x = a_0 B_0 \frac{(2EC_{\perp})^{1/2}}{\kappa E + B_0^2} \cos \xi_j \int_{-\pi/2}^{\pi/2} \cos \theta \cos \left[\frac{\theta}{\Omega_B} + \frac{2\theta - \sin(2\theta)}{4\Omega_E} \right] d\theta + \frac{a_0^2}{2(\kappa E + B_0^2)^{1/2}} \sin(2\xi_j) \int_{-\pi/2}^{\pi/2} \cos \left[\frac{2\theta}{\Omega_B} + \frac{2\theta - \sin(2\theta)}{2\Omega_E} \right] d\theta, \quad (17b)$$

where

$$\Omega_B = \frac{(\kappa E + B_0^2)^{3/2}}{C_\perp B_0^2}, \quad \Omega_E = \frac{(\kappa E + B_0^2)^{3/2}}{C_\perp \kappa E} \quad (18)$$

and ξ_j is the ‘‘time’’ of previous ‘‘collision’’.

In [23] it was shown that stochastic feature of ultrarelativistic electron dynamics described by Eq. (4, 7) but with $A_B = 0$, results in electron heating (depending on laser polarization) up to the energies

$$E_{\max}^y(B_0 = 0) \sim E_{\max}^{\text{abs}} \varepsilon^{6/7} \quad \text{and} \quad E_{\max}^x(B_0 = 0) \sim E_{\max}^{\text{abs}} \varepsilon^{12/11}. \quad (19)$$

We note that for $\varepsilon \ll 1$ both of these energies are below E_{\max}^{abs} but above the ponderomotive scaling.

Under the condition of $\Omega \ll 1$, we notice the fact that $|\theta| \ll 1$ mostly contributes to the integrals in equation (17), which enables the Taylor expansion of the terms in the square brackets of equations (17) as

$$\Omega_B^{-1} \theta + \Omega_E^{-1} [2\theta - \sin(2\theta)] / 4 \approx \Omega_B^{-1} \theta + \Omega_E^{-1} \theta^3 / 3, \quad (20)$$

and the integral limit can be extended to infinity. As a result, the integrals in equations (17a) and (17b) are degenerated to the Airy function $\text{Ai}(x)$ and its first derivative $\text{Ai}'(x)$, i.e.,

$$\Delta E_y \approx -2\pi a_0 \left(\frac{2EC_\perp}{\kappa E + B_0^2} \right)^{1/2} \Omega_E^{2/3} \sin \xi_j \text{Ai}'(\eta) + \frac{\pi a_0^2}{(\kappa E + B_0^2)^{1/2}} 2^{-1/3} \Omega_E^{1/3} \sin(2\xi_j) \text{Ai}(2^{2/3} \eta), \quad (21a)$$

$$\Delta E_x = 2\pi a_0 B_0 \left(\frac{2EC_\perp}{\kappa E + B_0^2} \right)^{1/2} \Omega_E^{1/3} \cos \xi_j \text{Ai}(\eta) + \frac{\pi a_0^2}{(\kappa E + B_0^2)^{1/2}} 2^{-1/3} \Omega_E^{1/3} \sin(2\xi_j) \text{Ai}(2^{2/3} \eta), \quad (21b)$$

where $\eta \equiv \Omega_E^{1/3} \Omega_B^{-1} = B_0^2 C_\perp^{2/3} (\kappa E)^{-4/3} / (1 + B_0^2 / \kappa E)$ and $B_0 \rightarrow 0$ (and thus $\Omega_B^{-1} \rightarrow 0$) provides the results in [23]. Considering the exponential decaying property of $\text{Ai}(x)$ and $\text{Ai}'(x)$ for $x > 1$, we see that efficient electron energy gain occurs for $\eta < \sigma$ ($\sigma \sim 1$ is a numerical factor) and thus $B_0^2 \ll \kappa E$. As a result we have $\Omega \approx \Omega_E$ and high- n resonances ($n\Omega = 1$) broadening and overlap are possible for $\Omega \ll 1$.

Ignoring the differences induced by $\text{Ai}(\eta)$, $\text{Ai}'(\eta)$ and $\text{Ai}(2^{2/3} \eta)$ which are in the same order, the condition of $|\Delta E| \ll E$ and thus $E \gg E_{\max}^{\text{abs}} \varepsilon^{3/2} = E_{\text{pond}} \varepsilon^{-1/2}$ (note that electron with small energy could also undergo stochastic heating but our analysis here is not applicable) assures that the first part on the right hand side (RHS) of equation (21a) is dominated [23]. As a result, we obtain

$$\Delta E_y \approx -2^{7/3} \pi \text{Ai}'(\eta) (E_{\max}^{\text{abs}})^{2/3} \varepsilon E^{1/3} \sin(\xi_j), \quad (22)$$

and $\eta \approx (B_0 / C_\perp)^2 (4E_{\max}^{\text{abs}} / E)^{4/3}$. The stochastic condition requires $K_y = |d\xi_{n+1} / d\xi_n - 1| \geq 1$ [16, 23], which reads

$$K_y = k_y \left(E_{\max}^{\text{abs}} / E \right)^{7/6} \varepsilon > 1, \quad (23)$$

where $k_y = -2^{4/3} \pi^2 \text{Ai}'(\eta)$ is a numerical factor. As a result, the decaying of $\text{Ai}'(\eta)$ with the increase of B_0 will cause a lower boundary for the stochastic electron energy depending on the magnetic strength. The maximum energy is slightly reduced from that without B_0 in equation

(19) (e.g., see the blue filled region in Fig. 2 where the red curve corresponds to $K_y = 1$). If we ignore the numerical factor $\sigma \sim 1$, then the stochastic electron motion approximately takes place in the energy space of $(B_0 C_\perp^{-1})^{3/2} < E / 4E_{\max}^{\text{abs}} < \varepsilon^{6/7}$ and thus for $B_0 > B_{\text{cri}} \equiv C_\perp \varepsilon^{4/7}$ there is no room for stochasticity.

However, for the laser polarized in x-direction, the first term on RHS of equation (21b) is present purely due to the magnetic field. As a result, this part could slightly increase the energy gain during each collision and thus the maximum stochastic energy shown in equation (19). The similar figure with Fig. 2 can be obtained for this case except that the approximately vertical line along the maximum stochastic energy has a tiny curvature toward large E for proper B_0 .

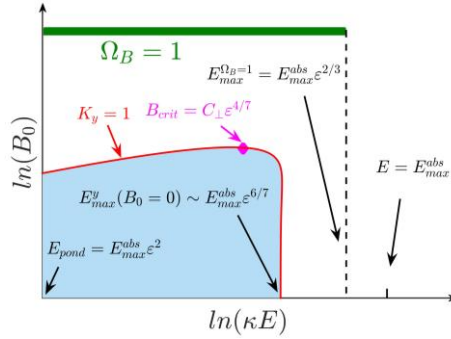


Fig. 2. Schematic view of the electron heating via the overlap of the resonances $n\Omega=1$ for high n (stochasticity in the blue filled region) for laser polarized along the static electric field and single resonance of $\Omega_B=1$ (green bar where the width has no meaning and it covers the energy $0 < E < E_{\max}^{\Omega_B=1}$) for both laser polarizations. The numerical factors order of unity for these maximum energies has been omitted.

In order to check these analyses, we performed numerical simulations to solve the 3/2D Hamiltonian equations and display the electron motion in the Poincaré mappings formed in the following way: it's on 2D energy E and laser phase $\Delta\xi$ ($0 < \Delta\xi < \pi$) space where $\Delta\xi \equiv \xi_n - m\pi$ with $m \equiv [\xi_n / \pi]$. E_n and ξ_n are picked from the center of the nonadiabatic regions as $\tilde{p}_y = 0$. Fig. 3 has shown the results of electron in the laser wave polarized along the transverse electric for $a_0 = 1$, $\kappa = 10^{-5}$, $C_\perp = 1$ and longitudinal magnetic field with (a) $B_0 = 0$, (b) $B_0 = 0.02$, and (c) $B_0 = 0.04$. From Fig. 3(b) we see a lower stochastic energy boundary while the maximum one remains unchanged. The termination of the stochasticity occurs around the critical magnetic field of $B_{\text{cri}} \approx 0.04$ as shown in Fig. 3(c) (we notice that $B_0 = 0.04$ is just below the critical magnetic field and any small increase of B_0 will result in regular electron motion). Shown in Fig.4 are the results for laser polarized along the x-direction with the parameters of $a_0 = 8$, $\kappa = 10^{-4}$, (a) $B_0 = 0$, and (b) $B_0 = 0.05$. We see the increase of the maximum stochastic energy for a proper B_0 in Fig. 4(b). For stronger magnetic field, the electron Poincaré mappings are similar to those in Fig. 3 (b, c). However, the difference between the stochastic electron motions due to the laser polarizations could be eliminated by adding relativistic momentum component of $\bar{P}_x \gg 1$ (e.g., see [23]) and so are the impacts of the magnetic field described above.

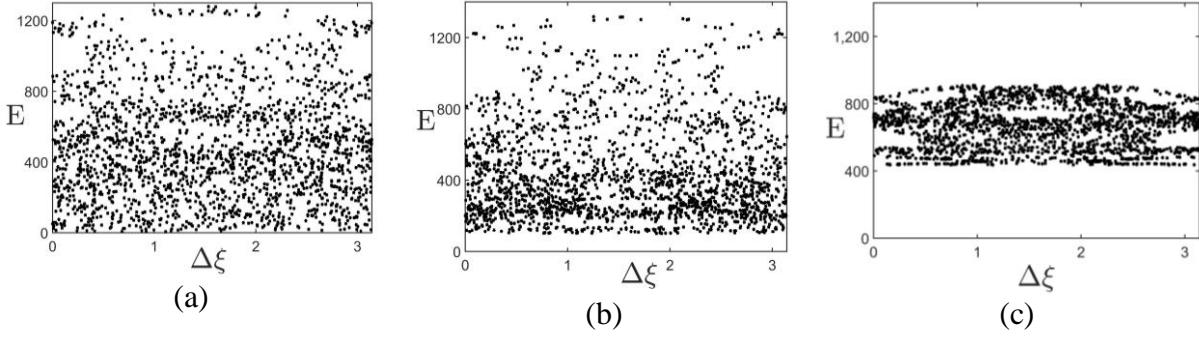


Figure 3. Poincaré mappings for electron moving in the laser wave polarized along the transverse electric for $a_0 = 1$, $\kappa = 10^{-5}$, $C_\perp = 1$ and longitudinal magnetic fields with (a) $B_0 = 0$, (b) $B_0 = 0.02$, and (c) $B_0 = 0.04$.

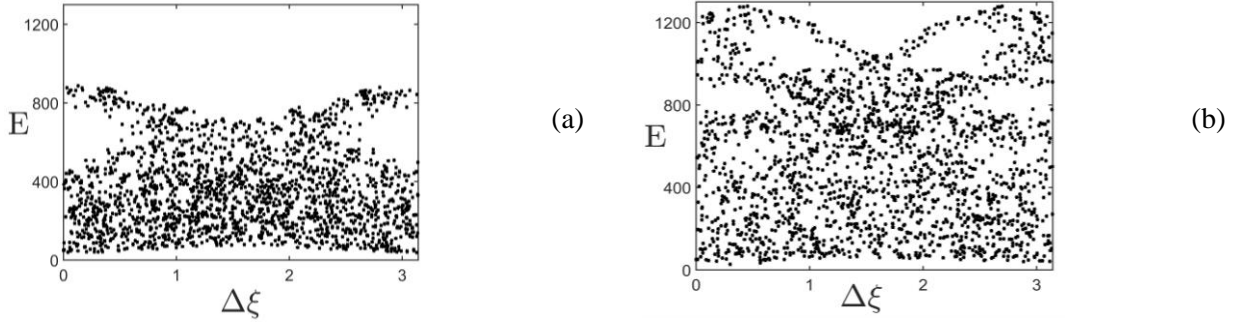


Figure 4. Poincaré mappings for electron moving in the laser wave polarized across to the transverse electric for $a_0 = 8$, $\kappa = 10^{-4}$ and longitudinal magnetic fields with (a) $B_0 = 0$ and (b) $B_0 = 0.05$.

5. Electron energy gains at low- n resonances

As shown in the previous section, for $B_0 \geq B_{\text{crit}}$ the stochastic heating mechanism will be terminated by the longitudinal magnetic field and the electron heating is only possible via single low- n resonance. For such resonant heating, we hope that the electron frequency $\Omega = 1/n$ in the static fields is mainly determined by Ω_B rather than by Ω_E such that there exists large room in electron energy space for electron being accelerated (otherwise the electron frequency Ω departs from the resonant condition $\Omega = 1/n$ quickly with the increase of E). Therefore, we consider the case of $B_0^2 \gg \kappa E$ and thus $\Omega \approx \Omega_B \approx B_0 / C_\perp$ in this section, where the initial match condition between the laser and cyclotron motion is of great importance [18].

Consider the condition of $\Omega \sim 1$, the electron laser interaction could be effective along the whole orbit shown in Fig. 1 for $E > E_{\text{pond}}$. However, we could still specify the time of electron passage through $y_{\text{max,min}}$ as ξ_j ($j=1,2,3,\dots$) such that the electron energy variation during this period can still be estimated by equations (17) but the equations (20-21) are not valid. By using the expansion of

$$e^{iz\sin\theta} = \sum_{m=-\infty}^{\infty} i^m J_m(z) e^{im\theta}, \quad (24)$$

where $J_{-m}(z) = (-1)^m J_m(z)$ is the m -th Bessel function of the first kind and $i^2 = -1$ [26], we obtain the energy variation as following:

$$\Delta E_y \approx \frac{\pi a_0 (E C_\perp)^{1/2}}{2^{1/2} B_0} J_{m=(\Omega_B^{-1} \pm 1)/2}(\rho) \sin \xi_j + \frac{\pi a_0^2}{2 B_0} J_{m=\Omega_B^{-1}}(2\rho) \sin(2\xi_j), \quad (25a)$$

$$\Delta E_x \approx \frac{\pi a_0 (E C_\perp)^{1/2}}{2^{1/2} B_0} J_{m=(\Omega_B^{-1} \pm 1)/2}(\rho) \cos \xi_j + \frac{\pi a_0^2}{4 B_0} J_{m=\Omega_B^{-1}}(2\rho) \sin(2\xi_j). \quad (25b)$$

where $\rho = (4\Omega_E)^{-1} \ll 1$. Considering the property of Bessel function as $\rho \rightarrow 0$, the efficient electron energy gain is only possible for $m=0$ ($\Omega_B = 1$ of $n=1$ resonance and thus $C_\perp = B_0$), where the difference of the energy change due to the laser polarization has disappeared.

From equations (25) we see that $\Delta E \propto E^{1/2}$ and it is continuously increasing without the transverse electric field. However, the presence of the transverse electric field, which induces a correction to the electron frequency of $|\Delta\Omega| \approx \kappa E / B_0^2$ as shown in equation (11), will set an upper limit to the resonant electron energy since after $m \approx 1/|\Delta\Omega|$ circles of cyclotron motion the sign of the energy gain (due to $\sin \xi_j$ or $\cos \xi_j$) in equation (25) changes. Then the maximum of the electron energy for $\Omega_B = 1$ can be estimated as

$$E_{\max}^{\Omega_B=1} \approx \frac{\pi^2 a_0^2 C_\perp}{2^3 B_0^2} \times m^2. \quad (26)$$

Taking $m = B_0^2 / 2\kappa \bar{E}$ where \bar{E} is the average energy which approximates to $\bar{E} = E_{\max}^{\Omega_B=1} / 2$, the maximum electron energy obtained from equation (26) reads

$$E_{\max}^{\Omega_B=1} \approx (2\pi)^{2/3} E_{\max}^{\text{abs}} \varepsilon^{2/3}. \quad (27)$$

For the small parameter $\varepsilon \ll 1$, this resonant energy is smaller than E_{\max}^{abs} but larger than the maximum stochastic energies shown in equation (19) (e.g., see Fig. 2 where the green bar is the energy region accessible to the resonant electron but its width has no meaning). The scaling of the maximum energy in equations (27) has been confirmed by the numerical results. For instance, shown in Fig. 5 are the electron energy and its trajectory versus time for $B_0 = C_\perp = 0.5$, $a_0 = 1$, $\kappa = 10^{-4}$ and initial conditions of $y = 0$ and $\tilde{p}_y = 0$.

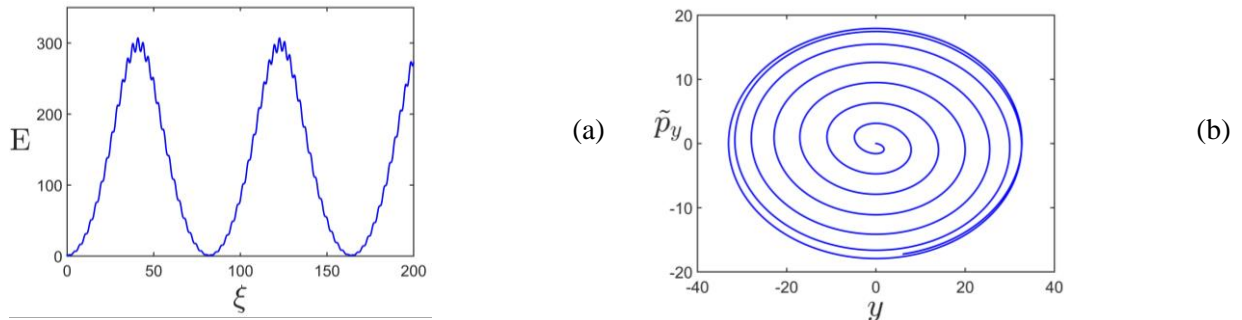


Figure 5. (a) Electron energy and (b) trajectory versus time $\xi = t - z$ for $B_0 = C_\perp = 0.5$; $a_0 = 1$, $\kappa = 10^{-4}$ and initial conditions $y = 0$, $p_y = p_x = 0$.

6. Conclusions

The 3/2 dimensional Hamiltonian method for electrons in the intense laser radiation and quasi-static transverse electric and longitudinal magnetic fields has been derived, within which the electron heating is examined both in the stochastic regime due to the overlap of broadened high harmonic resonances of electron frequency in weak electric and magnetic fields with the laser frequency, and for the low-n resonance for a strong longitudinal magnetic field. The maximum electron energy has been estimated for both cases. In the former case, the presence of a weak longitudinal magnetic field would reduce the maximum stochastic energy for laser polarized along the static electric field but slightly increase it for laser across to it with $\bar{P}_x = 0$. It also sets a lower boundary of stochastic electron energy until the stochasticity is terminated when the magnetic field exceeds a critical value $B_{\text{crit}} \sim C_{\perp} \varepsilon^{4/7}$. In the laser case, the efficient electron heating is only possible via the first harmonic resonance of $\Omega \approx \Omega_b \approx 1$. The maximum resonant energy, regardless the laser polarization, is above the maximum stochastic energy. All these energies in the measurement of ponderomotive scaling depend only on the parameter $\varepsilon \equiv \sqrt{2} a_0 \kappa^{1/2} C_{\perp}^{-3/2}$. Numerical simulations have been performed to confirm these results.

Acknowledgments. This work has been supported by the University of California Office of the President Lab Fee grant number LFR-17-449059.

References

- [1] Tajima T. and Dawson J. M. 1979 *Phys. Rev. Lett.* **42** 267
- [2] Rax J.-M. 1992 *Phys. Fluids B* **4** 3962
- [3] C. J. McKinstrie and E. A. Startsev 1997 *Phys. Rev. E* **56** 2130
- [4] Pukhov A. *et al* 1999 *Phys. Plasmas* **6** 2847
- [5] Gahn C. *et al* 1999 *Phys. Rev. Lett.* **83** 4772
- [6] Tsakiris G. D. *et al* 2000 *Phys. Plasmas* **7** 3017
- [7] Geyko V. I. *et al* 2009 *Phys. Rev. E* **80** 036404
- [8] Arefiev A. V. *et al* 2012 *Phys. Rev. Lett.* **108** 145004
- [9] Arefiev A. V. *et al* 2014 *Phys. Plasmas* **21** 033104
- [10] Robinson A. P. L. *et al* 2013 *Phys. Rev. Lett.* **111** 065002
- [11] Paradkar B. S. *et al* 2011 *Phys. Rev. E* **83** 046401
- [12] Paradkar B. S. *et al* 2012 *Phys. Plasmas* **19** 060703
- [13] Krasheninnikov S. I. 2014 *Phys. Plasmas* **21** 104510
- [14] Khudik V. *et al* 2016 *Phys. Plasmas* **23** 103108
- [15] A. V. Arefiev *et al* 2016 *Phys. Plasmas* **23** 056704
- [16] Zaslavskii G. M. *et al* 1987 *Sov. Phys. JETP* **66** 496
- [17] Liu B., *et al* 2013 *Phys. Rev. Lett.* **110**, 045002.
- [18] Arefiev A. V. *et al* 2015 *J. Plasma Phys.* **81** 475810404
- [19] Wu D. *et al* 2017 *Plasma Phys. Contr. Fusion* **59** 065004
- [20] Angus J. and Krasheninnikov S. I. 2009 *Phys. Plasmas* **16** 113103
- [21] Zhang Y. and Krasheninnikov S. I. 2018 *Phys. Plasmas* **25** 013120

- [22] Zhang Y. and Krasheninnikov S. I. 2018 *Physics Letters A* **382.27** 1801
- [23] Zhang Y., Krasheninnikov S. I. and Alexey Knyazev 2018 “*Stochastic electron heating in the laser and quasi-static electric and magnetic fields*”, submitted to *Phys. Plasmas*
- [24] R. Z. Sagdeev, D. A. Usikov, and G. M. Zaslavsky, *Nonlinear Physics: From the Pendulum to Turbulence and Chaos* (Hardwood Academic Publishers GmbH, Switzerland, 1988).
- [25] A. J. Lichtenberg and M. A. Lieberman, *Regular and chaotic Dynamics* (2nd Edition, Applied Mathematical Sciences, Vol. 38, New York, NY: Springer-Verlag, 1992).
- [26] L. D. Landau, E. M. Lifshitz, “The Classical Theory of Fields, V. 2, Course of Theoretical Physics”, Elsevier, 2009.